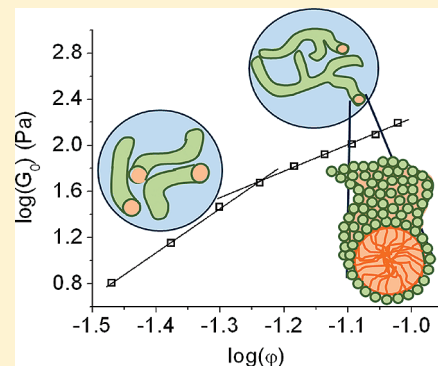


Unusual Scaling in the Rheology of Branched Wormlike Micelles Formed by Cetyltrimethylammonium Bromide and Sodium Oleate

Prasuna Koshy,^{†,‡} V. K. Aswal,[§] Meera Venkatesh,[‡] and P. A. Hassan^{*,†}[†]Chemistry Division, [‡]Radiopharmaceuticals Division, and [§]Solid State Physics Division, Bhabha Atomic Research Centre, Trombay, Mumbai 400 085, India

ABSTRACT: Natural fatty acids such as sodium oleate form highly viscous supramolecular complexes with long-chain cationic surfactants through cooperative self-assembly. Here we report the rheological behavior of linear and branched wormlike micelles formed in mixtures of cetyltrimethylammonium bromide (CTAB) and sodium oleate (NaOL). Addition of sodium oleate induces an increase in the axial ratio of the mixed micelles. At a constant mole fraction of the mixture, an increase in total surfactant concentration leads to a transition from linear to branched micelles. Both linear and branched micelles impart viscoelastic behavior to the fluid, and the low-frequency data can be approximated to the Maxwell model. Scaling of the rheological parameters of CTAB–NaOL catanionic mixtures, as a function of concentration, employing dynamic rheological measurements has been determined and compared with the predictions of existing scaling laws. The structural transition from linear micelles to the branched micelles in the CTAB–NaOL micellar system greatly influences the scaling behavior of shear modulus. The scaling exponent is lower for the branched micelles compared to linear micelles, analogous to those of linear and branched polymer melts. The structural evolution is probed by light scattering and small-angle neutron scattering measurements as well.



INTRODUCTION

The formation and properties of wormlike micelles in a surfactant system have drawn considerable interest in basic research and practical applications.¹ Due to their striking rheological properties, wormlike micelles have gained importance in a wide range of industrial applications such as fracturing fluids in oil fields, thickening of personal care products, and drag reduction in heat-transfer fluids.² When the number density of these wormlike micelles is sufficiently large, they entangle into a transient network leading to viscoelastic solutions that are analogous to that of semidilute polymer solutions.² These worm-like micelles are similar to polymers in that they are quite flexible and exhibit contour lengths of the order of micrometers.^{3,4} However, unlike classical polymers, wormlike micelles constantly break and recombine on a characteristic time scale. Hence, they do not exhibit a quenched contour length (molecular weight) distribution.

The scaling of rheological parameters of such wormlike micelles (WLMs) has been studied in detail by various groups and explained in terms of the reptation-reaction theory.⁵ Typically WLMs are formed by ionic surfactants in the presence of electrolytes or oppositely charged additives. This is because addition of salts or oppositely charged additives screens the electrostatic interaction between the charged head groups and allows closer packing of the surfactant monomers in the aggregate. This favors transition from spherical to cylindrical aggregates. One common feature in the rheology of such WLMs is that various ionic surfactants show a pronounced maximum of the zero-shear

viscosity as the salt/surfactant ratio is varied.^{6–11} This has been attributed to the formation of branched micelles at high salt to surfactant ratio. Direct observation of microstructures by cryo-transmission electron microscopy (cryo-TEM) in a variety of micelles beyond the viscosity maximum proved the existence of micellar branching. The scaling exponents of rheological parameters of entangled polymers have been shown to be sensitive to polymer topology. For example, comparing the rheological spectra of linear and star polymer melts shows widely differing properties. As opposed to linear polymers, a much broader range of relaxation time is observed for branched polymers.⁵ According to Cates et al., the rheological behavior of wormlike micelles follows simple scaling laws such as

$$\eta_0 \propto \varphi^{3.5}; \quad G_0 \propto \varphi^{2.25}$$

where η_0 is the zero-shear viscosity, G_0 the plateau modulus, and φ the volume fraction of the micelles.^{12–16} However, experimental results prove that the scaling law is applicable for nonionic wormlike surfactant systems. It has been reported that there is a deviation from this law for ionic WLMs, due to the electrostatic interactions among the constituent ionic surfactant moieties.¹⁷ However, there is no report on the dependence of the scaling of G_0 on the structural properties of the micellar system. No effort has been made so far to span the entire range of concentrations,

Received: June 9, 2011

Revised: July 22, 2011

Published: August 09, 2011

comprising both linear and branched micelles and a clear difference in the scaling behavior of shear modulus could be identified. Theoretical models developed to account for the viscosity of linear and branched micelles assumed a constant value of scaling exponents for the shear modulus. Here, we explore the rheological scaling of plateau modulus in a wormlike micellar fluid in the concentration range where linear and branched micellar transition occurs. Typically, WLMs are formed by the addition of oppositely charged hydrotropes or surfactants to an ionic micellar solution. Surfactant mixtures will be the preferred choice over hydrotropes for this study, because there is a possibility of changes in the composition of mixed micelles in the case of surfactant–hydrotrope mixtures. This is due to the fact that hydrotropes, alone, do not form any aggregates at low concentration, and hence the composition of hydrotropes in the micelles can vary with concentration. Rheological studies on the viscoelastic fluids comprising long-chain cationic alkyltrimethylammonium bromide and hydrophobic counterions or anionic surfactants have already been reported by other groups.^{18–27} The hydrocarbon chain length of the alkyltrimethylammonium bromides (C_n TAB) affects the rheology of C_n TAB–sodium oleate (NaOL) mixtures as reported by Raghavan et al.²⁸ They hypothesized the occurrence of the maximum in the viscosity plot of NaOL– C_8 TAB mixtures as a function of total surfactant concentration is due to the formation of branched micelles. Later Cui et al. have demonstrated through cryo-TEM imaging that the maximum in the shear viscosity is due to the transition from linear to branched micelles.²⁹ In our study, NaOL has been selected as the anionic surfactant for the formation of catanionic micelles in conjunction with cationic CTAB solution. Our selection of NaOL was based on the fact that, with NaOL being a surfactant, there is minimal possibility of it being leached out of the mixed micelles upon dilution, as opposed to hydrotropes. Hence, rheological parameters of a given mole fraction can be investigated over a wide range of concentrations. With this aim, a detailed rheological study on the CTAB–NaOL catanionic mixture was done to determine the effect of structural transition on the rheological parameters of the mixed micelles.

In this paper, we report the rheological behavior of WLMs in a cationic–anionic mixture formed by CTAB and NaOL. A detailed concentration dependence on the shear modulus of the catanionic mixture was investigated with the help of rheological measurements. The aim of our study is to compare the scaling behavior of linear and branched micelles and to investigate if the scaling exponent is different for linear and branched micelles, as observed in certain polymer melts. With the help of DLS and SANS measurements, microstructural changes have been investigated in CTAB solutions by the addition of NaOL, in the presence as well as in the absence of electrolyte NaCl.

EXPERIMENTAL SECTION

A. Materials and Methods. CTAB was obtained from SD Fine Chem Ltd., Mumbai, India, and NaOL and sodium chloride were obtained from Sigma Aldrich. All chemicals were used as received without further purification. Deionized water from a Millipore-Milli-Q system (resistivity $\sim 18\text{ M}\Omega\text{ cm}$) was used to prepare all of the aqueous solutions, and the samples were equilibrated for 48 h at 25 °C before measurements were done at neutral pH.

B. Rheology. Rheological measurements were conducted at 25 °C using an Anton Paar Physica MCR 101 rheometer in a double gap concentric cylinder geometry (DG 26.7) with a Peltier temperature control. The shear rate investigated was from 0.1 to 200 s^{-1} .

C. Small-Angle Neutron Scattering. Small angle neutron scattering (SANS) experiments were carried out using small-angle neutron scattering diffractometer at the Dhruva reactor, Bhabha Atomic Research Centre, Trombay, India.³⁰ The diffractometer makes use of a beryllium oxide filtered beam with a mean wavelength (λ) of 5.2 Å. The angular distribution of the scattered neutrons is recorded using a one-dimensional (1D) position-sensitive detector (PSD). The accessible wave vector transfer ($q = 4\pi \sin \theta / \lambda$, where 2θ is the scattering angle) range of the diffractometer is 0.017–0.35 Å^{−1}. The PSD allows simultaneous recording of data over the full q . The samples were held in a quartz sample holder of 0.5 cm thickness. In all of the measurements the temperature was kept fixed at 30 °C. The measured SANS data have been corrected and normalized to absolute unit (as cross-section per unit volume), using standard procedures.

THEORETICAL BACKGROUND

A. Rheological Behavior. In the semidilute regime the viscoelastic behavior of the entangled micelles is reminiscent of that of polymeric networks. One important difference in the transient character of a micellar solution from a “dead” polymeric network is that the micelles can break and recombine on a characteristic time scale. The dynamics of such a “living” polymer solution was studied in detail by Cates and co-workers.^{15,31,40} This model involves two relevant time scales that are the reptation time, τ_{rep} , and the breaking time, τ_b . The reptation time corresponds to the curvilinear diffusion of a chain of mean length \bar{L} along a tube that is constrained by the entanglements from other chains and the breaking time is the mean time required for a chain of length \bar{L} to break into two pieces. It is assumed that the chemical relaxation process is the reversible unimolecular scission characterized by a temperature-dependent rate constant k_1 per unit arc length per unit time, which is the same for all elongated micelles and is independent of time and the volume fraction. This assumption results in

$$\tau_b = (k_1 \bar{L})^{-1} \quad (1)$$

For $\tau_b \gg \tau_{\text{rep}}$, the dominant stress relaxation mechanism is reptation. Then the stress relaxation function indeed obeys the equation¹⁵

$$\mu(t) \sim \exp(-t/\tau_{\text{rep}})^{1/4} \quad (2)$$

Thus, in this regime the terminal relaxation time $\tau_R = \tau_{\text{rep}}$.

The zero shear viscosity η_0 is related to τ_R and the plateau modulus G_0 by the relation

$$\tau_R = \eta_0 / G_0 \quad (3)$$

When $\tau_b \ll \tau_{\text{rep}}$, an interesting new regime occurs. In this regime, chain breakage and recombination will both occur often, before it reptates out of the tube segment. The stress relaxation is then characterized by a new intermediate time scale, $\tau_R = (\tau_b \tau_{\text{rep}})^{1/2}$, associated with a process whereby the chain breaks at a point close enough to a given segment of tube for reptation relaxation of that segment to occur before a new chain end is lost by

recombination. Thus, at low frequencies the behavior of the liquid is Maxwellian and is described by the equations

$$G'(\omega) = \frac{(\omega\tau_R)^2}{1 + (\omega\tau_R)^2} G_0 \quad (4)$$

$$G''(\omega) = \frac{\omega\tau_R}{1 + (\omega\tau_R)^2} G_0 \quad (5)$$

where G_0 is the plateau modulus and $\tau_R = \eta_0/G_0$ is the relaxation time. The Cole–Cole representation, in which the imaginary part $G''(\omega)$ of the frequency-dependent shear modulus is plotted against the real part $G'(\omega)$, can be used to get an estimate of the relaxation time, τ . Thus, at low frequencies, the Maxwellian behavior is ascertained by a semicircular shape of the Cole–Cole plot $G''(G')$, but deviations from the half-circle occur at a circular frequency, ω , of the order of the inverse of the breaking time of the micelles. The model of Granek and Cates¹³ can also be applied to study the regimes involving small time scales where the dominant polymer motion is not reptation but either breathing (which arises from the tube length fluctuations) or the local Rouse-like motion (arising from stretches of chain shorter than the entanglement length, l_e), characterized by an apparent turn up of both $G'(\omega)$ and $G''(\omega)$ at high frequencies. This results in a minimum in the G'' vs G' plot and extrapolation of G' to x -axis yields G'_∞ . This picture applies when l_e is much larger than the persistence length, l_p , and the breaking time is much larger than the Rouse time, τ_e . It was found that, provided $\tau_b \gg \tau_e$, the value of $G''(\omega)$ at the dip obeys the relation

$$G''_{\min}/G'_\infty = l_e/\bar{L} \quad (6)$$

From the values of G''_{\min} , G'_∞ , and l_e one can thus obtain an estimate of micellar length, \bar{L} . For flexible micelles l_e can be estimated from the relation³²

$$G'_\infty = k_B T / \xi^3 = k_B T / l_e^{9/5} l_p^{6/5} \quad (7)$$

where ξ is the correlation length.

B. Small-Angle Neutron Scattering. The differential scattering cross-section per unit volume ($d\Sigma/d\Omega$) as a function of scattering vector q , for a system of charged, monodispersed interacting particles, could be written as

$$\frac{d\Sigma}{d\Omega} = n(\rho_m - \rho_s)^2 V^2 [\langle F(q)^2 \rangle + \langle F(q) \rangle^2 (S(q) - 1)] + B \quad (8)$$

where n denotes the number density of micelles, ρ_m and ρ_s are the scattering length densities of the micelle and the solvent, respectively, and V is the micelle volume. $F(q)$ is the single-particle form factor, and $S(q)$ is the interparticle structure factor. B is a constant term, which represents the incoherent scattering background. The single-particle form factor has been calculated by treating the micelles as prolate ellipsoids, using the equations

$$\langle F(q)^2 \rangle = \int_0^1 [F(q, \mu)^2 d\mu] \quad (9)$$

$$\langle F(q) \rangle^2 = \int_0^1 [F(q, \mu) d\mu]^2 \quad (10)$$

$$\langle F(q, \mu) \rangle = \frac{3(\sin x - x \cos x)}{x^3} \quad (11)$$

$$x = q[a^2\mu^2 + b^2(1-\mu^2)]^{1/2} \quad (12)$$

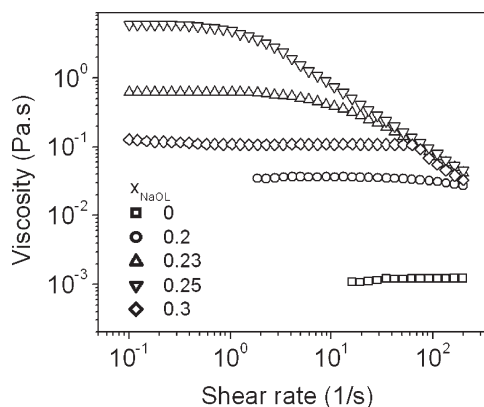


Figure 1. Viscosity, η , of CTAB–NaOL mixtures (total surfactant concentration, $C_T = 0.1$ M) as a function of shear rate at different mole fractions of sodium oleate (x_{NaOL}).

where a and b are the semimajor and semiminor axes of an ellipsoidal micelle, respectively, and μ is the cosine of the angle between the directions of a and the wave vector transfer q . The interparticle structure factor $S(q)$ specifies the correlation between the centers of different micelles, and it is the Fourier transform of the radial distribution function $g(r)$ for the mass centers of the micelle. We calculated $S(q)$ using expressions derived by Hayter and Penfold from the Ornstein–Zernike equation and using the rescaled mean spherical approximation.³³ The micelle is assumed to be a rigid equivalent sphere of diameter $\sigma = 2(ab^2)^{1/3}$ interacting through a screened Coulomb potential. The micelle dimensions, aggregation number, and fractional charge were determined from this analysis. In the absence of intermicellar interaction, a model-independent analysis of the data can be performed using indirect Fourier transformation, which provides the pair distance distribution function. The Fourier transformation is performed using the program GENOM developed by Svergun.³⁴

RESULTS AND DISCUSSION

NaOL is a well-known surfactant for its high interfacial activity. It has been applied in many fields such as being one of the main constituents of cell membranes, useful for biological applications and also can be used as collectors in the flotation deinking of paper and minerals.^{35,36} The presence of a long hydrocarbon chain with an unsaturation makes it conducive for the formation of complex catanionic aggregates without phase separation.³⁷ CTAB–NaOL mixtures form viscoelastic fluids over a wide range of composition and concentration. Under appropriate conditions, linear or branched WLMs are formed in CTAB–NaOL mixtures, without precipitation of the catanionic salt. Traditionally, the existence of branched micelles has been hypothesized from a decrease in the viscosity of the fluid with an increase in mole fraction or concentration. First, we identify the microstructural evolution from steady shear rheology. Figure 1 shows the shear-dependent viscosity of CTAB–NaOL micelles (total surfactant concentration is 100 mM) at different mole fractions of NaOL (x_{NaOL}). At lower x_{NaOL} , viscosity is independent of shear rate; i.e., Newtonian flow behavior is observed in the studied shear range. When the mole fraction is above 0.2, the Newtonian behavior occurred at low shear rates only and shear thinning is observed at large deformations, when the shear

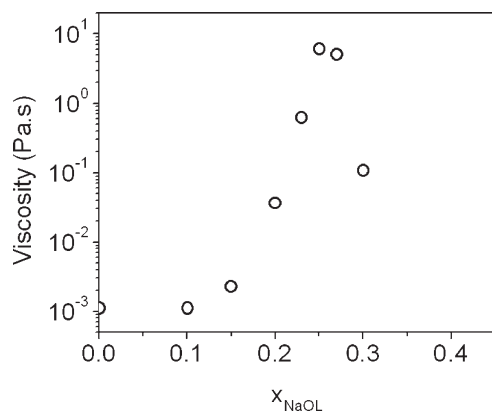


Figure 2. Variation of the zero-shear viscosity, η_0 , of CTAB–NaOL mixed micelles with varying x_{NaOL} ($C_T = 0.1$ M).

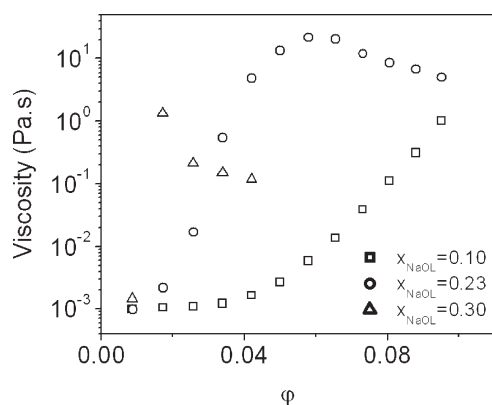


Figure 3. Variation of zero-shear viscosity of CTAB–NaOL mixed micelles as a function of micelle volume fraction (ϕ) at $x_{\text{NaOL}} = 0.1, 0.23$, and 0.3 .

rate exceeds a critical value. With an increase in x_{NaOL} up to a value of 0.25, the critical shear rates for shear thinning shift gradually to lower values. However, with further increase in x_{NaOL} , again higher deformation rates are required to induce shear thinning. The zero shear viscosity, i.e., viscosity plateau at low shear rates, as a function of x_{NaOL} is depicted in Figure 2. The zero shear viscosity is comparable to that of water at low x_{NaOL} , which increases to a maximum, nearly 4 orders of magnitude higher than that of water and then again decreases with increasing x_{NaOL} . This rheological behavior is typical of a wormlike micellar system exhibiting a structural transition from linear to branched micelles. At a given volume fraction, the viscosity of branched micelles is lower than that of linear micelles, as the branch points can slide along the length of the micelles, providing an additional mechanism for stress relaxation.

To understand the concentration scaling of the rheological parameters of CTAB–NaOL catanionic mixtures, linear and dynamic rheological measurements were performed on the mixed micelles as a function of the volume fraction of micelles, at fixed x_{NaOL} . Variation of zero shear viscosity at three different mole fractions of sodium oleate, 0.1, 0.23, and 0.3, as a function of the volume fraction of micelles (ϕ) is depicted in Figure 3. The mole fractions of the mixed micelles are chosen such that the compositions span different regimes in the viscosity plot, viz., below, near, and above the viscosity maximum. For $x_{\text{NaOL}} = 0.1$,

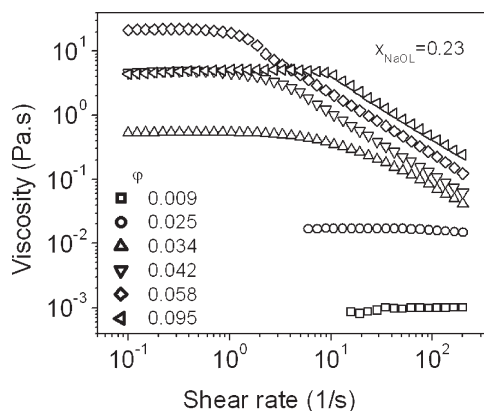


Figure 4. Shear viscosity versus shear rate for CTAB–NaOL mixed micelles with varying ϕ , at a fixed $x_{\text{NaOL}} = 0.23$.

the viscosity change is marginal at low ϕ values, suggesting very small growth and low number density of the mixed micelles. An increase in the viscosity occurs at $\phi \approx 0.05$ and continues to increase in a linear manner. This increase in viscosity above a critical volume fraction indicates transition from a dilute to a semidilute regime of ellipsoidal micelles. In the semidilute regime, the viscosity varies linearly with the volume fraction. This observed linear scaling behavior indicates that no structural transition has occurred in the studied concentration range. This suggests that, for $x_{\text{NaOL}} = 0.1$, short ellipsoidal micelles retain their structure with an increase in ϕ , with a mere increase in the number density of micelles. However, the behavior is different at higher mole fractions of sodium oleate, $x_{\text{NaOL}} = 0.23$ and 0.3 . At $x_{\text{NaOL}} = 0.23$, the viscosity increases even at low ϕ and a linear increase in the viscosity is observed only up to a particular value of ϕ ; thereafter, the viscosity decreases slowly. Occurrence of the semidilute regime even at low volume fraction indicates that the micelles are long. The decrease in viscosity at very high ϕ values indicates a transition from linear to branched micelles. This indicates that, at this mole fraction, a slight change in concentration favors the formation of branched micelles and hence the viscosity decreases with concentration. From the initial steady shear data, it is inferred that the mole fraction of 0.23 is ideal for exploring the scaling of rheological parameters of both linear and branched micelles, as it spans both regimes. At low volume fractions, mostly linear micelles are formed, while, at high volume fractions, only branched micelles are favored.

Another feature in the rheology of WLMs is their deviation from Newtonian behavior. Figure 4 depicts the shear-dependent viscosity at a constant mole fraction of sodium oleate, $x_{\text{NaOL}} = 0.23$, at different volume fractions of micelles. At low ϕ , the system shows Newtonian behavior. With increasing ϕ , the catanionic mixture shows shear thinning behavior at large deformations. With further increase in ϕ , shear thinning occurs at lower shear rates and zero shear viscosity increases as already discussed above. At this mole fraction, long polymer-like micelles are preferred to spherical micelles and the number density of the WLMs increases with an increase in ϕ , forming a network structure. The network structure of the catanionic mixture is deformed by applying a shear, and shear thinning occurs due to the alignment of aggregates under flow, if the deformation is faster than the time required for regaining equilibrium network structure. Also relaxation becomes slower with an increase in network structure, explaining shear thinning at lower shear rates.

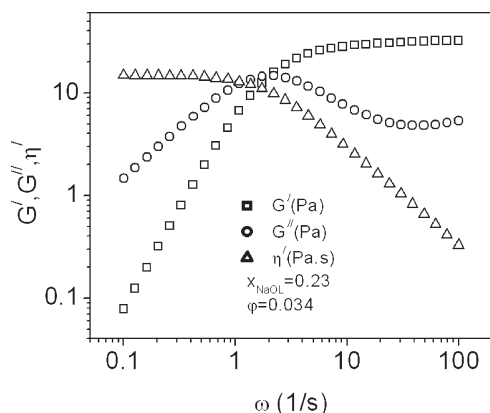


Figure 5. Variation of the storage modulus (G'), loss modulus (G''), and real part of the complex viscosity (η') as a function of frequency (ω) at 25 °C for a CTAB–NaOL mixture. $x_{\text{NaOL}} = 0.23$, and $\phi = 0.034$.

At large ϕ , CTAB–NaOL mixtures again start exhibiting shear thinning behavior at large deformations with a decrease in viscosity, suggesting the formation of branched micelle. Note that, here, the linear to branched micelle transition is induced by a change in volume fraction of the micelles. With increasing ϕ , the spontaneous interfacial curvature of aggregate decreases, increasing the energy cost for the formation of hemispherical end-caps of the cylindrical micelles. The end-cap energy can be minimized if the free ends of the cylindrical micelles fuse with cylindrical part of its own or other micelles, thus developing into branched WLMs. When stress is applied, such micellar joints can slide along its cylindrical body (contour), thereby allowing a fast stress relaxation process. This is consistent with the recent report on sodium oleate–octyltrimethylammonium bromide (C_8TAB) mixtures by Chellamuthu and Rothstein.³⁸ At a fixed molar ratio, 70/30, of NaOL to C_8TAB , the shear rheology measurements showed a maximum in shear viscosity at 4 wt % followed by a sharp decrease in viscosity with increasing total surfactant concentration. With the help of cryo-TEM, it was concluded that the maximum in shear viscosity for these fluids corresponds to the transition from linear entangled to branched micelles. The branched micelles eliminate the strain hardening due to the ghostlike crossing of the two entangled WLMs and the sliding of branch points along the length of a wormlike micelle.

The dynamic rheology of WLMs has been explored in detail, in the past decades, both in linear and branched micelle regimes. The scaling exponents of the zero shear viscosity and the stress relaxation time show marked difference during transition from linear to branched micelles. However, no significant changes in the scaling exponents of plateau moduli are reported so far. This is contrary to the reports on melt rheology of branched polymers, which suggest that the introduction of branching leads to a decrease in the plateau modulus. The limited concentration range over which branched micelles exists restricts precise determination of the scaling exponents in the branched micelle regime. In certain cases, identification of a well-defined plateau in the storage modulus becomes difficult due to overlap of the Rouse mode. To investigate the scaling of rheological parameters in linear and branched regimes, dynamic rheological measurements were performed on CTAB–NaOL catanionic mixtures with varying ϕ . All measurements were restricted to the mole fraction of 0.23. Figure 5 shows the variation of storage and loss modulus, G' and G'' , respectively, as a function of frequency ω ,

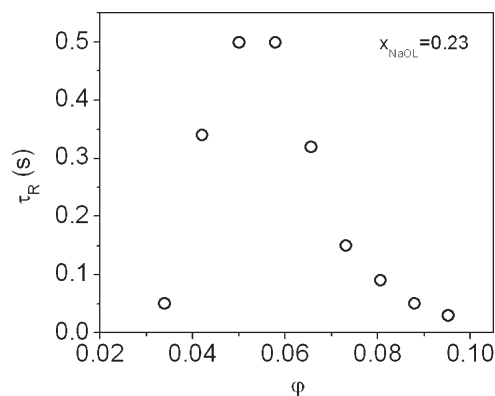


Figure 6. Variation of the stress relaxation time (τ_R) of CTAB–NaOL mixtures as a function of ϕ at a fixed $x_{\text{NaOL}} = 0.23$.

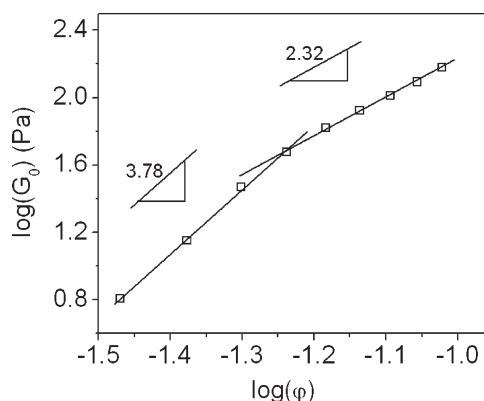


Figure 7. Variation of logarithm of the plateau modulus (G_0) as a function of logarithm of volume fraction of CTAB–NaOL micelles, at a fixed $x_{\text{NaOL}} = 0.23$. A change in the slopes of the graph indicates change in the scaling exponent.

for $\phi = 0.034$ at 298 K. It can be seen that the solution shows typical viscoelastic behavior, as G' varies as ω^2 and G'' varies as ω , at low frequencies. $G'(\omega)$ and $G''(\omega)$ cross each other at an intermediate frequency, i.e., crossover frequency (ω_R). Assuming that the behavior is close to the Maxwell model, the relaxation time and plateau modulus can be obtained from the values of modulus and frequency at the crossover point. The stress relaxation time (τ_R) is obtained as the reciprocal of the crossover frequency, while the plateau modulus can be taken as twice the value of the modulus at the crossover point. Figure 6 depicts variation of τ_R with ϕ of micelles. With increasing ϕ , there is an increase in τ_R followed by a maximum around $\phi \approx 0.06$. With further increase in ϕ , τ_R decreases after reaching a maximum, indicating the structural transition to branched micelles as already discussed. A plot of $\log(G_0)$ as a function of $\log(\phi)$ has been depicted in Figure 7. One can clearly identify two distinct regimes, consistent with the linear and branched regimes as inferred from viscosity data. A linear plot is obtained up to $\phi \approx 0.05$ with a slope of 3.78. For $\phi > 0.05$, the slope of the plot changes to 2.32. This clearly suggests that the scaling exponents of G_0 for linear and branched micelles are significantly different. Moreover, the exponent for branched micelles is lower than that of linear micelles, as is the case with polymer melts. Recently the scaling behavior of different wormlike mixed micelles, including sodium decanote (SD)/CTAB, sodium laurate (SL)/CTAB,

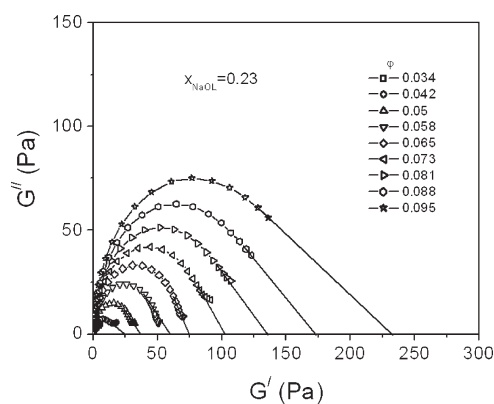


Figure 8. Variation of G'' as a function of G' at different volume fractions of CTAB–NaOL micelles at a fixed $x_{\text{NaOL}} = 0.23$. The solid lines show an extrapolation of the high-frequency data to obtain G'_∞ .

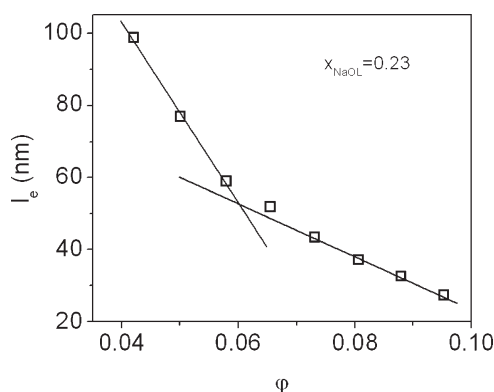


Figure 9. Variation of l_e as a function of volume fraction of CTAB–NaOL micelles, at a fixed $x_{\text{NaOL}} = 0.23$.

sodium didecaminocystine (SDDC)/CTAB, and sodium dilauroaminocystine (SDLC)/CTAB, has been investigated by Fan et al. and the results have been compared with the Cates model.¹² It has been shown that the scaling behavior is influenced by the surfactant structure and the mixing ratios. Such behavior is mainly due to the electrostatic interactions between the WLMs, i.e., the charge density of WLMs, regardless of the surfactant structure. The Cates model is applicable when the charge density of the WLMs is below a threshold value, regardless of the possible changes in the chain packing. The presence of electrostatic interactions can significantly affect the scaling exponents. The preparation and structure–property behavior of linear and branched thermoplastic poly(urethane ureas) (TPUUs) and polyureas with different soft segments have been investigated. A comparison of the rheological behavior of linear and branched polymers suggest that the hyperbranched polymers show a lower plateau modulus as compared to linear polymers.³⁹

Figure 8 shows the variation of G' and G'' , in the form of Cole–Cole plots (at different ϕ), and attempts were made to fit the data using the Maxwell model employing G_0 and τ_R reported above. It was found that at low frequencies the Maxwell model fits reasonably well to the data (fit not shown). However, at high frequencies the plateau modulus deviates from the value expected from the Maxwell model. Alternately, the exact value of the plateau modulus can be obtained from an extrapolation of the Cole–Cole plot to the x -axis, as shown in the figure. The

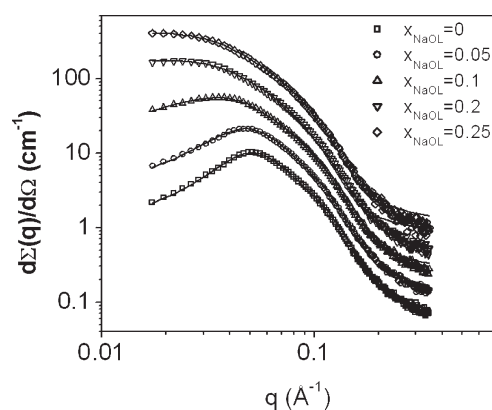


Figure 10. SANS spectra for CTAB–NaOL mixtures ($C_T = 0.1$ M) at different x_{NaOL} . The data for $x_{\text{NaOL}} = 0$ are absolute values, while the remaining plots are offset by a factor of 2 for clarity. The solid lines are fit to the data using a model for charged ellipsoids, as discussed in the text.

variation of G'_∞ , obtained by such an extrapolation, also shows different scaling exponents in the two regimes, negating the possibility of biased errors in the estimation. From G'_∞ , we can calculate l_e for the flexible micelles using eq 7. Figure 9 depicts entanglement length as a function of the volume fraction of micelles, assuming the value of persistence length of the CTAB–NaOL micellar system to be 200 Å.⁴⁰ It can be observed that the slope of the graph changes with the structural transition from linear to branched micelles, which is in line with the G_0 vs ϕ graph. This also supports our study of changes in the scaling behavior of the rheological parameters with the structural transition in the micellar system.

■ MICELLAR GROWTH PROBED BY SANS AND DLS

SANS is an ideal tool to assess the structural polymorphism in surfactant assemblies due to the large scattering contrast that can be achieved by using deuterated solvents. Though the linear and branched micelles cannot be differentiated from the SANS analysis, the structural evolution from spherical to elongated micelles can be assessed in a quantitative manner by SANS analysis. SANS spectra of mixed micelles at different x_{NaOL} , at a total surfactant concentration of 100 mM, are depicted in Figure 10. A characteristic correlation peak at intermediate q appears for pure 100 mM CTAB solution, indicating electrostatic interaction between the micelles as they are positively charged. With an increase in x_{NaOL} , the correlation peak broadens and also shifts to lower q values. It also shows an increase in intensity at low q , with an increase in x_{NaOL} . The broadening in the correlation peak indicates a decrease in the range of electrostatic interactions. The increase in the intensity at low q region suggests a growth in the micellar structure. To obtain structural parameters of the micelles, the SANS spectra were modeled as charged prolate ellipsoids interacting through a screened Coulomb potential.⁴¹ Fractional charge, semimajor axis, and semiminor axis are used as the variables in the fit. It was noted that, in order to obtain good fit, a polydispersity in the semimajor axis was necessary and has been included using Schultz distribution. In all samples a polydispersity parameter $z = 35$ was used in the semimajor axis. The aggregation number was calculated from the relation $N = 4\pi ab^2/3v$, where v is the surfactant monomer volume, estimated using the Tanford formula. The experimental data fit reasonably well with the model, and the parameters of the

Table 1. Micellar Parameters Obtained from the SANS Analysis of 0.1 M CTAB–NaOL Mixed Micelles with Varying Mole Fraction of Sodium Oleate

sample no.	x_{NaOL}^a	N_{agg}^b	α^c	b^d (Å)	a^e (Å)	axial ratio
1	0	157	0.14	21.4	49.3	2.3
2	0.05	188	0.09	22.4	53.9	2.4
3	0.1	335	0.01	23.2	88.1	3.8
4	0.2	497	0.01	26.4	96.3	3.6
5	0.25	947	0.01	25.6	199.9	7.8

^a x_{NaOL} = mole fraction of sodium oleate. ^b N_{agg} = aggregation number. ^c α = fractional charge. ^d b = semiminor axis. ^e a = semimajor axis.

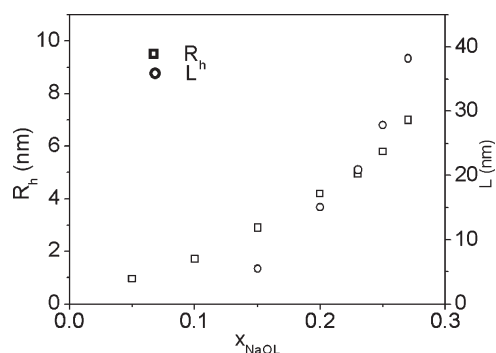


Figure 11. Variation of apparent hydrodynamic radius (R_h) and micellar length (L) of CTAB–NaOL mixed micelles ($C_T = 0.1$ M) at different x_{NaOL} .

fit are summarized in Table 1. With an increase in x_{NaOL} , the axial ratio of the micelles increases and the fractional charge decreases. It suggests the possibility of transition from nearly spherical to rodlike micelles.

Changes in the microstructure of CTAB micelles upon addition of sodium oleate have also been probed by dynamic light scattering. Figure 11 depicts the apparent hydrodynamic radius (R_h) of a CTAB–NaOL cationic mixture as a function of increasing x_{NaOL} . Apparent hydrodynamic radius, deduced using the Stokes–Einstein equation, increases with increasing x_{NaOL} . At low x_{NaOL} , R_h is consistent with the value of that of spherical micelles. However, with an increase in x_{NaOL} , the equivalent sphere diameter of the micelles increases and it reaches a value inconsistent with the alkyl chain length of the surfactant. This suggests growth of the globular micelles to form anisotropic aggregates. Cationic micelles can grow either as disklike (oblate) or rodlike (prolate) micelles. Rheology and SANS have already indicated the structural transition from spherical to rodlike micelles. Also, the apparent diffusion coefficient, D_a , can be related to the length of the rod and its axial ratio, L/d , by Broersma's relationship given as⁴²

$$D_0 = \frac{k_B T}{3\pi\eta L} \left[\ln\left(\frac{L}{d}\right) + \zeta \right] \quad (13)$$

where k_B is the Boltzmann constant, T the absolute temperature, η the solvent viscosity, and ζ the shape factor, a function of the axial ratio L/d using the expressions of Tirado et al., which are valid for axial ratios in the range of 4–30, given as⁴³

$$\zeta = 0.312 + 0.5656/(L/d) - 0.05/(L/d)^2 \quad (14)$$

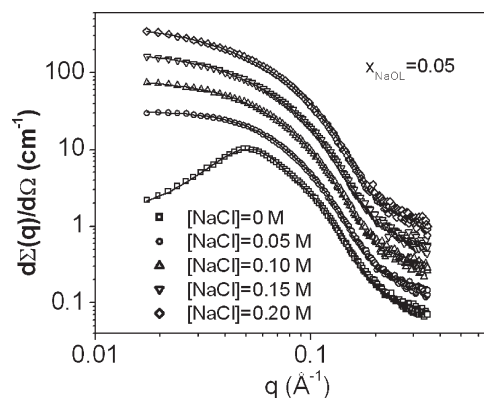


Figure 12. SANS spectra for CTAB–NaOL mixed micelles at a fixed $x_{\text{NaOL}} = 0.05$ and varying concentration of NaCl. The spectra of $x_{\text{NaOL}} = 0.05$ in the absence of NaCl are absolute values, while the remaining plots are offset by a factor of 2 for clarity. The solid lines are fit to the data using ellipsoidal micelles.

Translational diffusion coefficient alone cannot give both the length and the diameter of the rodlike micelles. Hence, fixing the diameter of the rodlike micelles as twice the length of the hydrocarbon chain of the surfactant, the length of the rodlike micelles is calculated using an iterative procedure as depicted in Figure 11. The length of the micelles varies from a few nanometers to about 35 nm, as x_{NaOL} varies from 0 to 0.27. At small x_{NaOL} , D_a could not be analyzed using the above relationship, suggesting that the axial ratio is smaller than 4. It has been observed that, at high mole fractions, the micellar length estimated from DLS is significantly larger than that obtained from SANS. This is primarily because of the fact that at high mole fractions, when the charge density of the micelles is low, the micelles are highly polydisperse with an exponential length distribution. Due to the limited Q -range of SANS, the features are primarily from the small segments of the long micelles, or short rods; while DLS results will be skewed to longer micelles, as it measures the z -average diffusion coefficient. Moreover, in entangled micellar solutions, the micellar length estimated from DLS will be an upper estimate due to restricted diffusion of the micelles.

A. Effect of Electrolyte. Though the observed deviation in the scaling exponent of plateau modulus, at high surfactant concentration, occurs at a concentration where branched micelles are formed, the possibility of changes in the electrostatic interactions or flexibility of the micelles cannot be ruled out. This is because of the fact that an increase in the concentration of surfactants leads to an increase in the counterion concentration and hence can affect the growth behavior due to variation in the ionic strength of the medium. This effect is more pronounced when the surface charge of the micelles is rather high. We investigated the effect of ionic strength on these mixed micelles using NaCl as the electrolyte. SANS spectra for NaOL–CTAB mixed micelles, at constant $x_{\text{NaOL}} = 0.05$ ($C_T = 100$ mM), with varying concentration of NaCl is shown in Figure 12. Considering the fact that a small amount of counterion variation will have little effect on neutral micelles, we kept the mole fraction of mixed micelle at 0.05 so that the micelles do remain as charged. In the absence of NaCl, the spectrum shows a correlation peak, indicating the presence of repulsive intermicellar interaction between the cationic micelles, arising due to a net positive charge on the micelles. With the addition of NaCl, the correlation peak is less

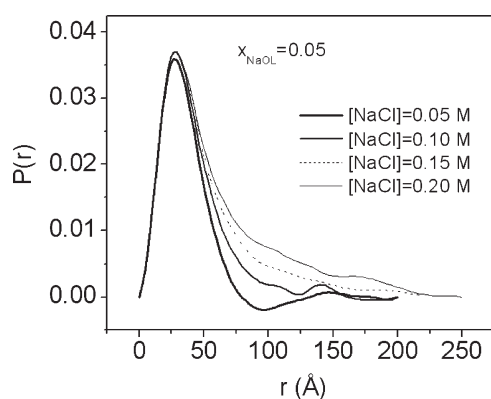


Figure 13. PDDFs (obtained from the IFT analysis of the SANS spectra) of CTAB–NaOL mixed micelles at a fixed $x_{\text{NaOL}} = 0.05$ and varying concentration of NaCl.

Table 2. Micellar Parameters Obtained from the SANS Fit for 0.1 M CTAB–NaOL Mixed Micelles with Varying NaCl Concentration at a Fixed Mole Fraction of Sodium Oleate ($x_{\text{NaOL}} = 0.05$)

sample no.	[NaCl] (M)	N_{agg}^a	α^b	b^c (Å)	a^d (Å)	axial ratio
1	0	188	0.09	22.4	53.9	2.4
2	0.05	279	0.01	22.6	78.6	3.5
3	0.1	278	0.01	22.6	77.6	3.4
4	0.15	313	0.01	22.0	92.2	4.2
5	0.2	345	0.01	21.6	105.9	4.9

^a N_{agg} = aggregation number. ^b α = fractional charge. ^c b = semi-minor axis. ^d a = semimajor axis.

pronounced, which indicates interparticle interaction between the micelles is negligible. The added electrolyte has effectively screened the electrostatic repulsion. With increasing NaCl concentration, forward scattering also increases, suggesting growth of the micelles. We first employed the model-independent IFT method, to assess the structural changes, as intermicellar interaction is relatively weak in the presence of NaCl. The IFT method allows us to evaluate the pair distance distribution function (PDDF), $p(r)$, of the micelles. Variations in the $p(r)$ function of the micelles with increasing NaCl concentration, as obtained from the IFT analysis, are depicted in Figure 13. The PDDF of mixed micelles composed of $x_{\text{NaOL}} = 0.05$ ($C_T = 100$ mM), in the low electrolyte concentration shows the influence of structure factor, $S(q)$ (though weak), as indicated by a weak oscillation in $p(r)$. With increasing NaCl concentration of the mixed micelles, this oscillation disappears and the micelles continuously transform into short rods with increasing average length. On the basis of the structural information obtained from IFT analysis, the SANS data were fitted using a prolate ellipsoid model. In the presence of NaCl, no interparticle interaction is taken into account. The experimental data fits reasonably well with the model, and the parameters of the fit are summarized in Table 2.

At low salt concentration, the axial ratio of the micelles increases with increasing electrolyte concentration, as salt produces the screening effect in the catanionic mixture. It should be noted that the growth of the catanionic mixture is very large when the mole fraction of sodium oleate is increased compared to the growth of the catanionic mixture with

increasing electrolyte concentration. Once the interactions are screened, further addition of NaCl produces very little changes in the aggregation number. This suggests that the effect of electrolytes on neutral micelles is negligible and hence the observed changes in the shear modulus arise mainly from branching of the micelles. Addition of nonpenetrating counterions such as NaCl results in small growth of the catanionic mixed micelles, due to the screening effect or by decreasing the charge density of the micelles. But the addition of penetrating oleate (OL^-) ion binds strongly to the CTA^+ ions, and hence the growth is in the form of giant WLMs. Recently Gokul et al. have compared the growth behavior of NaOL in the presence of a binding salt (triethylammonium chloride, Et_3NHCl) and simple salt (potassium chloride, KCl). Both salts promote the growth of micelles. A simple salt such as KCl showed a growth of the micelles from spherical to worm-like micelles but binding salt like Et_3NHCl also modifies the phase behavior of NaOL solution. There is cloud point behavior in solutions of NaOL and Et_3NHCl , attributed to the onset of attractive interactions between the anionic micelles at high temperatures due to strong binding of the counterions.⁴⁴ The contour lengths and flexibility of long micelles are greatly influenced by the chemical structure of the additives. The role of electrostatic and specific ion binding in tuning the contour lengths and the flexibility of the mixed micelles of cetyltrimethylammonium 2,6-dichlorobenzoate and cetyltrimethylammonium chloride as a function of surfactant and salt concentrations has been reported by Magid et al.⁴⁵ Addition of highly hydrated, nonpenetrating electrolyte such as NaCl salt will form small and globular micelles over a wide range of surfactant and salt concentrations. However, addition of less hydrated, penetrating counterions such as 2,6-dichlorobenzoate form giant WLMs even at low concentrations of hydrophobic counterions. Increasing the composition of penetrating counterions of the catanionic pair lowers the 1D bending modulus of the micelles and increases their flexibility.⁴⁵ However, the effect of these parameters on shear modulus appears to be minimal, and the observed variation in shear modulus clearly suggests different scaling for linear and branched micelles.

CONCLUSION

We monitored the rheological behavior of CTAB–NaOL mixed micelles over a wide concentration range exhibiting both linear and branched micelles. The aim of our study is to understand the scaling behavior of linear and branched micelles and identify if there is any difference in the scaling exponents, as in the case of polymers. Due to the presence of a long hydrocarbon chain with an unsaturated bond in anionic oleate moiety, CTAB–NaOL mixtures form viscoelastic fluids over a wide range of composition and concentration. Hence, under appropriate conditions, linear or branched wormlike micelles are formed in CTAB–NaOL mixtures, without precipitation of the catanionic salt. Small-angle neutron scattering, dynamic light scattering, and rheological measurements suggest the microstructural transition from sphere to rodlike to wormlike micelles with an increase in the mole fraction of sodium oleate in the CTAB–NaOL mixed micelles. Steady flow rheological measurements indicate Newtonian behavior when the axial ratio of the micelles is small, while non-Newtonian (shear thinning) behavior is observed when the micelles are long enough to form entangled structures. Dynamic rheology of

the entangled micelles is similar to Maxwell fluids, which is one of the basic models for a viscoelastic fluid. According to Cates et al., the rheological behavior of wormlike micelles follows simple scaling laws. Concentration dependence study of CTAB–NaOL mixed micelles at a fixed mole fraction of sodium oleate ($x_{\text{NaOL}} = 0.23$) has shown that the exponents in the scaling laws change when the structural transition occurs from linear to branched micelles. The slope in the graph of plateau modulus vs volume fraction of the CTAB–NaOL micelles change from 3.78 to 2.32 when the structural transition occurs from linear to branched micelles. This is different from what is predicted by Cates and others. Most of the reports on WLMs suggested a constant scaling exponent for linear and branched micelles, and no attempts have been made so far to account for any changes in the shear modulus of linear and branched micelles. Our studies indicate that the scaling exponents for branched micelles of the catanionic surfactant system agrees well with the values predicted by theoretical models, while for linear micelles an increase in the exponent is observed. Also the slope of the plot of entanglement length vs volume fraction of the micelles shows an abrupt change in the linear to branched micelle regime. This rheological behavior of the mixed micelles is analogous to the polymer melts, as previous studies report that a comparison of the rheological behavior of linear and branched polymers suggests that the hyperbranched polymers show a lower plateau modulus as compared to linear polymers. It appears that there is a need to develop more robust theories to explain the shear modulus of linear and branched micelles. Systematic studies on dynamic rheology of branched and linear micelles for a wide range of surfactant systems are needed to identify scaling exponents.

AUTHOR INFORMATION

Corresponding Author

*Tel.: + 91- 22 25595099. Fax: + 91- 22 25505151. E-mail: hassan@barc.gov.in.

REFERENCES

- (1) Zana, R.; Kaler, E. W. *Giant micelles: Properties and applications*; Vol. 140; CRC Press: New York, 2007.
- (2) Ezrahi, S.; Tuvai, E.; Aserin, A. *Adv. Colloid Interface Sci.* **2006**, 128–130, 77–102.
- (3) Cates, M. E.; Candau, S. J. *J. Phys. Condens. Matter* **1990**, 2, 6869–6892.
- (4) Amin, S.; Kermis, T. W.; Zanten, R. M. V.; Dees, S. J.; Zanten, J. H. V. *Langmuir* **2001**, 17, 8055–8061.
- (5) McLeish, T. C. B. *Adv. Phys.* **2002**, 51, 1379–1527.
- (6) Raghavan, S. R.; Kaler, E. W. *Langmuir* **2001**, 17, 300–306.
- (7) Cappelaere, E.; Cressely, R. *Colloid Polym. Sci.* **1998**, 276, 1050–1056.
- (8) Schubert, B. A.; Kaler, E. W.; Wagner, N. J. *Langmuir* **2003**, 19, 4079–4089.
- (9) Khatory, A.; Lequeux, F.; Kern, F.; Candau, S. J. *Langmuir* **1993**, 9, 1456–1464.
- (10) Candau, S. J.; Khatory, A.; Lequeux, F.; Kern, F. *J. Phys. IV* **1993**, 3, 197–209.
- (11) Oelschlaeger, C.; Suwita, P.; Willenbacher, N. *Langmuir* **2010**, 26, 7045–7053.
- (12) Fan, H.; Yan, Y.; Li, Z.; Xu, Li.; Zhang, B.; Huang, J. *J. Colloid Interface Sci.* **2010**, 348, 491–497.
- (13) Graneck, R.; Cates, M. E. *J. Chem. Phys.* **1992**, 96, 4758–4767.
- (14) Turner, M. S.; Cates, M. E. *J. Phys. II* **1992**, 2, 503–519.
- (15) Cates, M. E. *Macromolecules* **1987**, 20, 2289–2296.
- (16) Drye, T. J.; Cates, M. E. *J. Chem. Phys.* **1992**, 96, 1367–1375.
- (17) Koehler, R. D.; Raghavan, S. R.; Kaler, E. W. *J. Phys. Chem. B* **2000**, 104, 11035–11044.
- (18) Rehage, H.; Hoffmann, H. *J. Phys. Chem.* **1988**, 92, 4712–4719.
- (19) Shikata, T.; Hirata, H.; Kataoka, T. *Langmuir* **1989**, 5, 398–405.
- (20) Clausen, T. M.; Vinson, P. K.; Minter, J. R.; Davis, H. T.; Talmon, Y.; Miller, W. G. *J. Phys. Chem.* **1992**, 96, 474–484.
- (21) Appell, J.; Porte, G.; Khatory, A.; Kern, F.; Candau, S. J. *J. Phys. II* **1992**, 2, 1045–1052.
- (22) Hayashi, S.; Ikeda, S. *J. Phys. Chem.* **1980**, 84, 744–751.
- (23) Anet, F. A. L. *J. Am. Chem. Soc.* **1986**, 108, 7102–7103.
- (24) Soltero, J. F. A.; Puig, J. E.; Manero, O.; Schulz, P. C. *Langmuir* **1995**, 11, 3337–3346.
- (25) Kaler, E. W.; Herrington, K. L.; Murthy, A. K.; Zasadzinski, J. A.; Chiruvolu, S. *J. Phys. Chem.* **1993**, 97, 13792–13802.
- (26) Brasher, L. L.; Herrington, K. L.; Kaler, E. W. *Langmuir* **1995**, 11, 4267–4277.
- (27) Yacilla, M. T.; Herrington, K. L.; Brasher, L. L.; Kaler, E. W.; Zasadzinski, J. A. *J. Phys. Chem.* **1996**, 100, 5874–5879.
- (28) Raghavan, S. R.; Fritz, C.; Kaler, E. W. *Langmuir* **2002**, 18, 3797–3803.
- (29) Cui, H.; Hodgdon, T. K.; Kaler, E. W.; Abezgauz, L.; Danino, D.; Lubovsky, M.; Talmon, Y.; Pochan, D. **2007**, 3, 945–955.
- (30) Aswal, V. K.; Goyal, P. S. *Curr. Sci.* **2000**, 79, 947–953.
- (31) Cates, M. E.; Turner, M. S. *Europhys. Lett.* **1990**, 11 (7), 681–686.
- (32) Berret, J. F.; Appell, J.; Porte, G. *Langmuir* **1993**, 9, 2851–2854.
- (33) Hayter, J. B.; Penfold, P. J. *J. Mol. Phys.* **1981**, 42, 109–118.
- (34) Svergun, D. I. Mathematical methods in small-angle scattering data analysis. *J. Appl. Crystallogr.* **1991**, 24, 485–492.
- (35) Park, J.; An, K.; Hwang, Y.; Park, J. G.; Noh, H. J.; Kim, J. Y.; Park, J. H.; Hwang, N. M.; Hyeon, T. *Nat. Mater.* **2004**, 3, 891–895.
- (36) Croce, V.; Cosgrove, T.; Flood, C.; Dreiss, C. A.; Karlsson, G. *Langmuir* **2005**, 21, 7646–7652.
- (37) El-Kadi, N.; Martins, F.; Clausse, D.; Schulz, P. C. *Colloid Polym. Sci.* **2003**, 281, 353–362.
- (38) Chellamuthu, M.; Rothstein, J. P. *J. Rheol.* **2008**, 52 (3), 865–884.
- (39) Unal, S.; Yilgor, I.; Yilgor, E.; Sheth, J. P.; Wilkes, G. L.; Long, T. E. *Macromolecules* **2004**, 37, 7081–7084.
- (40) Hassan, P. A.; Candau, S. J.; Kern, F.; Manohar, C. *Langmuir* **1998**, 14, 6025–6029.
- (41) Aswal, V. K.; Goyal, P. S. *Physica B* **1998**, 245, 73–80.
- (42) Lehner, D.; Lindner, H.; Glatter, O. *Langmuir* **2000**, 16, 1689–1695.
- (43) Tirado, M. M.; Martinez, C. L.; de La Torre, J. G. *J. Chem. Phys.* **1984**, 81, 2047–2052.
- (44) Kalur, G. C.; Raghavan, S. R. *J. Phys. Chem. B* **2005**, 109, 8599–8604.
- (45) Magid, L. J.; Han, Z.; Li, Z. *J. Phys. Chem. B* **2000**, 104, 6717–6727.